

CCAR-1 works together with the U2AF large subunit UAF-1 to regulate alternative splicing

Doreen I. Lugano, Lindsey N. Barrett, Dale Chaput, Margaret A. Park, and Sandy D. Westerheide

Department of Cell Biology, Microbiology, and Molecular Biology, University of South Florida, Tampa, FL, USA

ABSTRACT

The Cell Division Cycle and Apoptosis Regulator (CCAR) protein family members have recently emerged as regulators of alternative splicing and transcription, as well as having other key physiological functions. For example, mammalian CCAR2/DBC1 forms a complex with the zinc factor protein ZNF326 to integrate alternative splicing with RNA polymerase II transcriptional elongation in AT-rich regions of the DNA. Additionally, *Caenorhabditis elegans* CCAR-1, a homolog to mammalian CCAR2, facilitates the alternative splicing of the perlecan *unc-52* gene. However, much about the CCAR family's role in alternative splicing is unknown. Here, we have examined the role of CCAR-1 in genome-wide alternative splicing in *Caenorhabditis elegans* and have identified new alternative splicing targets of CCAR-1 using RNA sequencing. Also, we found that CCAR-1 interacts with the spliceosome factors UAF-1 and UAF-2 using mass spectrometry, and that knockdown of *ccar-1* affects alternative splicing patterns, motility, and proteostasis of UAF-1 mutant worms. Collectively, we demonstrate the role of CCAR-1 in regulating global alternative splicing in *C. elegans* and in conjunction with UAF-1.

ARTICLE HISTORY

Revised 15 November 2023
Accepted 17 November 2023

KEYWORDS

C. elegans; alternative splicing; CCAR-1; UAF-1; RNA sequencing

1. Introduction


The human cell requires hundreds of thousands of proteins but contains approximately 30,000 genes [1–3]. To overcome this impediment, the alternative splicing (AS) of mRNAs allows one gene to produce multiple isoforms of a protein, causing an expansion of the proteome [4–10]. This process occurs in 70% of human genes and is facilitated by members of the spliceosome, *cis*-acting sequences, and *trans*-acting factors [4–6,11].


The human cell division cycle apoptosis regulator (CCAR) family of proteins is involved in many aspects of cell physiology, including metabolism, apoptosis, stress response regulation, alternative splicing, and transcription [12–19]. This ability to participate in multiple processes is likely due to the presence of various structural domains, including an S1-like RNA binding domain, a nuclear localization domain, a leucine zipper domain, a Nudix domain, and an EF-hand domain [13]. The mammalian CCAR1 leucine zipper domain interacts with members of the NF- κ B family of transcription factors [20], whereas the Nudix domain is thought to bind metabolites such as NAD⁺ and acts as an inactive holdase [12]. The coiled-coiled domain is predicted to be involved in protein-protein interactions [13], and the EF-hand domain is an inactive variant of a calcium-dependent regulatory domain [21–23].

An emerging function of the CCAR family is in the regulation of alternative splicing. Mammalian CCAR2 forms

a complex with zinc factor ZNF326, forming the DBIRD complex which binds both RNA polymerase II and the ribonucleoprotein particle [24]. This interaction with the DBIRD complex integrates alternative splicing with RNA polymerase II elongation and is most prevalent in A/T-rich regions of the DNA [24]. Interestingly, this process is independent of SIRT1, a histone deacetylase that is known to regulate CCAR2 [24]. Here, we use *C. elegans* as a model organism in order to learn more about the mechanism of CCAR proteins in alternative splicing. *C. elegans* is an excellent model for studying alternative splicing due to the conservation of the splicing machinery, the ability to manipulate the worm genetically, and the availability of viable splicing factor mutants [8,9,13]. In addition, there is high conservation of the CCAR protein family structure within species, with mammalian CCAR2 having 30% sequence similarity to *Caenorhabditis elegans* CCAR-1 [13].

We use RNA sequencing analysis to show genome-wide alternative splicing changes that occur with the deletion of CCAR-1 in *C. elegans*. Additionally, using mass spectrometry, we show that CCAR-1 interacts with spliceosome factors UAF-1 and UAF-2. Furthermore, we demonstrate that *ccar-1* RNAi affects the alternative splicing patterns and motility of UAF-1 mutants. Finally, we show that *ccar-1/uaf-1* RNAi reduces the amount of polyglutamate aggregates in a *C. elegans* Huntington's disease model worm. Altogether, our study demonstrates the role of CCAR-1 in global alternative splicing changes in *C. elegans* and its role in

CONTACT Doreen I. Lugano  doreenikhuva@usf.edu  Department of Cell Biology, Microbiology, and Molecular Biology, University of South Florida, 4202 E. Fowler Ave ISA 2015, Tampa, FL 33620, USA

 Supplemental data for this article can be accessed online at <https://doi.org/10.1080/15476286.2023.2289707>

© 2023 The Author(s). Published by Informa UK Limited, trading as Taylor & Francis Group.

This is an Open Access article distributed under the terms of the Creative Commons Attribution-NonCommercial License (<http://creativecommons.org/licenses/by-nc/4.0/>), which permits unrestricted non-commercial use, distribution, and reproduction in any medium, provided the original work is properly cited. The terms on which this article has been published allow the posting of the Accepted Manuscript in a repository by the author(s) or with their consent.

conjunction with UAF-1 in regulating alternative splicing at the organismal level.

2. Materials and methods

2.1. *C. elegans* strains and maintenance

The following strains were used in the study: Wild-type Bristol N2, VC1029 *ccar-1* (gk433) IV, MT16492 *uaf-1*(n4588) III, VC3010 *uaf-2* (gk3159) IV, AM140 *rmls132* (*unc-54p::Q35::YFP*) and SDW080 (*peft::CCAR-1::GFP::3×flag*). All strains were maintained at 20°C on standard NGM plates seeded with *Escherichia coli* OP50–1. Synchronous populations of nematodes were obtained by bleach synchronization and plating for 19 hours on NGM plates without food.

The VC1029 *ccar-1* (gk433) IV strain was acquired from CGC (*Caenorhabditis elegans* Genetic Centre) and outcrossed three times to our laboratory N2 wildtype strain to generate the SDW040 strain. SDW080 transgenics were constructed by PCR amplification of the full-length *ccar-1* gene followed by subsequent Gibson assembly to insert a GFP reporter and a ubiquitous *eft* promoter. The homologous repair template was then injected at a final concentration of 10ng/μl at Knudra Transgenics (Murray, UT). Successful transgene insertion was detected by fluorescence of GFP and western blotting.

AM140 (*rmls132* [*unc-54p::Q35::YFP*]) are Huntington disease model worms with 35 Polyglutamine (polyQ) residues, tagged to YFP. PolyQ expansions are defined as the cause of cellular toxicity in neurodegenerative diseases such as Huntington's disease. In *C. elegans* young adults with 35–40 glutamine residues exhibit protein aggregates and loss of motility [25]. MT16492 *uaf-1*(n4588) III and VC3010 *uaf-2* (gk3159) IV are UAF-1 and UAF-2 mutant worms obtained from CGC, that are previously used to study functions of these genes in the alternative splicing of *C. elegans* [26].

2.2. RNA preparation for RNA sequencing

RNA samples were prepared using a Trizol reagent (Ambion). The concentration and purity of RNA were determined using Nanodrop Spectrometry and further QC on the RNA and library were assessed at the Brigham Young University DNA sequencing centre. RNA libraries were prepared using the TruSeq Total RNA kit (Illumina, Inc.) with a Ribo-zero gold kit (Illumina, Inc.) to remove rRNA and mitochondrial RNA transcripts.

2.3. VAST-Tools analysis

Vertebrate Alternative Splicing and Transcription Tools (VAST-Tools) was used to identify alternative splicing events from our RNA-Seq data [27–29]. VAST-Tools is a powerful tool that profiles and compares alternative splicing events from RNA-Seq data by aligning to species-specific library files known as VASTDB. The output from the alignment allows users information on alternative splicing events [28].

We used paired-end next-generation data to determine differential exon skipping, intron retention, alternative splice

donor, and alternative splice acceptor between N2 and SDW040 worms. VAST-Tools was run with default parameters using *vast-tools align*, *vast-tools combine*, and *vast-tools diff* to the *C. elegans* genome (*vastdb.cel.23.06.20*). Alternative splicing events were reported in a tab file containing statistical changes and a PDF file plotting of the splicing changes. For the analysis of significantly changing genes, we used a cut-off $E[dPSI] < 0.1$ and $MV [dPSI] > 0$. Gene ontology of significantly alternatively spliced genes was done using WormEnrichR [30,31].

2.4. RT-PCR

RNA samples were prepared using Trizol reagent (Ambion) followed by cDNA synthesis using SuperScript III reverse transcriptase kit (Invitrogen). For the cDNA synthesis 250 ng of RNA per sample was used and subsequently, 300 ng of the cDNA was used in the PCR reaction.

The samples were amplified through conventional PCR with designed primers, spanning 200–800 base pairs of each gene. The primers were specifically designed to identify splicing changes between alternative exons and introns. We used the following primers for the *F10F8.10* gene, forward primer: GATGGAAGGAACTGCTAGA and reverse primer: CCA TCAAATAATCCAGTCGAC and forward primer: ATCTACGGATTCGAGTCGTCACCATC and reverse primer: GAAGAAATCTTCCAGTCCGAAGGG for the *tos-1* gene.

The PCR samples were separated in a 5% TBE polyacrylamide gel [32], and stained with SYBR gold nucleic acid stain (Invitrogen). The gel images were taken by Molecular Imager F.X. (Bio-Rad), and the densitometries of the bands were calculated through Image J for quantitation.

2.5. Thrashing assay

The worms were synchronized and then grown in desired OP50–1/RNAi plates until the fourth larval stage. On day 1 of adulthood, individual worms were placed in a drop of nematode growth media on the lid of a petri dish. The number of body bends by each worm per minute was recorded. This was repeated for 15 worms per condition, where*** is a p-value of < 0.0001 and ** is a p-value of < 0.005 based on Mann-Whitney statistical tests.

2.6. Protein aggregation assay

AM140 (*Q35::YFP*) worms were grown in desired RNAi plates until the fourth larval stage. Worms were picked to fresh plates until day 3 of adulthood. Protein aggregates were imaged using the EVOS fluorescent microscope for at least 15 worms per condition in independent biological triplicates.

2.7. Mass spectrometry

SDW080 (*peft::CCAR-1::GFP::3×flag*) worms were maintained at 20°C on standard NGM plates seeded with *Escherichia coli* OP50–1. Immunoprecipitation was performed by pulldown of CCAR-1 using GFP in biological duplicates to generate eluates for mass spectrometry.

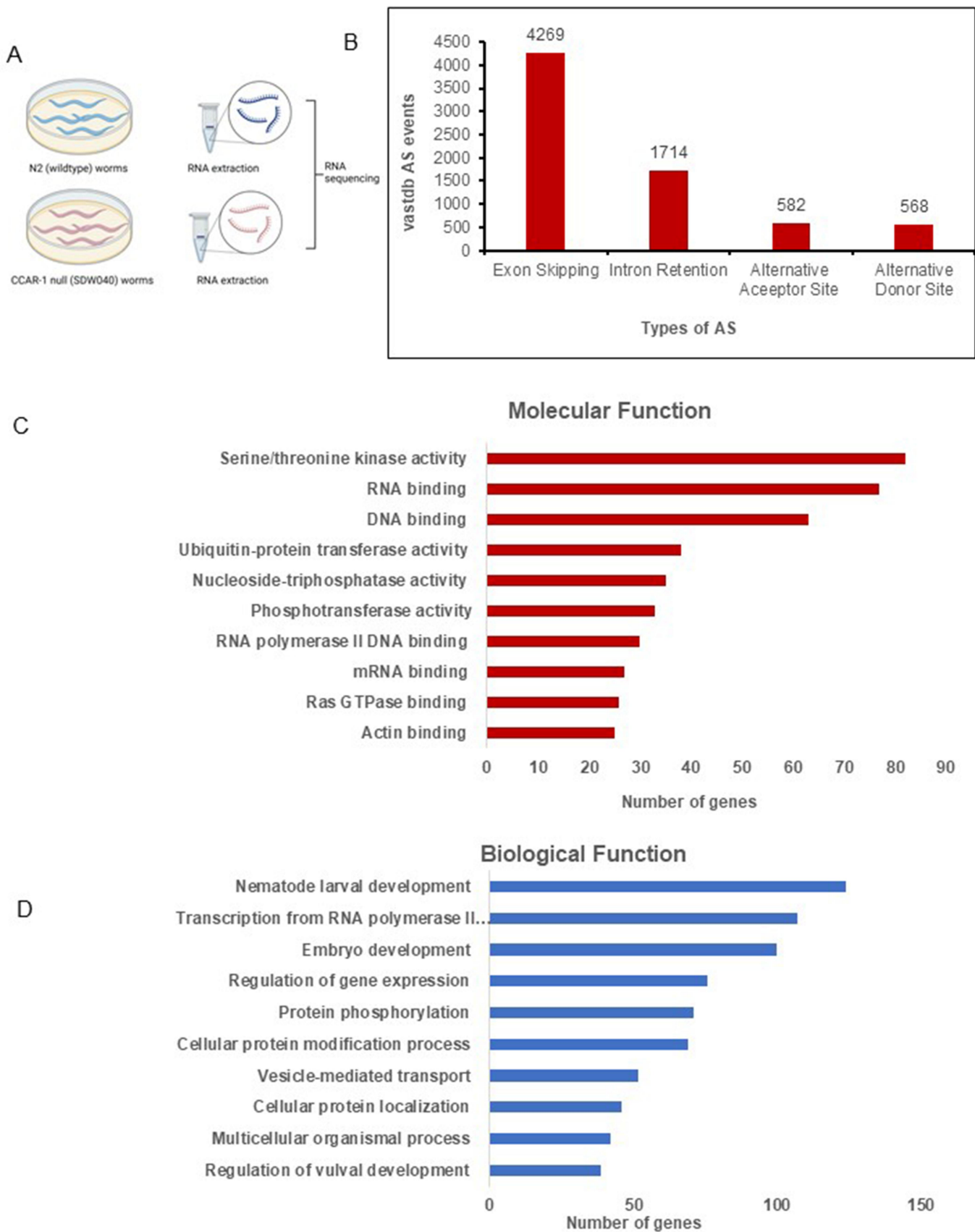


Figure 1. CCAR-1 regulates alternative splicing. **A.** Methodology of RNA sequencing samples preparation between N2 and CCAR-1 null (SDW040) worms. **B.** Types of alternative splicing events occurring from the VAST Tools analysis, including exon skipping (EX), intron retention (INT), alternative splice acceptor (ALTA) and alternative splice donor (ALTD). **C.** WormEnrichR analysis of gene ontology (GO) molecular function between N2 and CCAR-1 null (SDW040) worms. **D.** WormEnrichR analysis of gene ontology (GO) biological process between N2 and CCAR-1 null (SDW040) worms.

Table 1. Top 20 alternatively spliced genes between N2 (wildtype) and CCAR-1 null (SDW040) worms.

<i>Caenorhabditis elegans</i> genes	Human homolog	Alternative splicing event	Function
srap-1	MACF1	Exon Skipping	Human microtubule actin crosslinking factor 1 (MACF1), crosslinks actin to other cytoskeletal proteins and also binds microtubules.
trr-1	TRRAP	Alternative Splice Acceptor	Involved in the negative regulation of vulval development, positive regulation of growth rate and reproduction.
unc-82	NUAK1	Exon Skipping	Serine threonine kinase important for maintaining myosin filament organization.
rskn-1	RPS6KA1	Alternative Splice Acceptor	Ribosomal protein S6 kinase involved in signal transduction and protein phosphorylation.
F13H8.5	N/A	Exon Skipping	Enriched in ADE sheath, germline precursor cell and hypodermis.
sax-7	L1CAM	Intron Retention	Conserved transmembrane cell adhesion molecule involved in development of distinct neurone, dendrite development, and axon guidance.
lea-1	KIAA1881	Exon Skipping	Protects cells against various abiotic stresses such as high salinity, desiccation and heat and cold stress.
F30F8.10	NAA60	Intron Retention	Enables histone acetyltransferase activity and peptide alpha-N-acetyltransferase activity.
T24B8.7	ENSP00000385700	Alternative Splice Acceptor	Enables cysteine-type deubiquitinase activity and cysteine-type endopeptidase activity.
apr-1	APC	Alternative Splice Acceptor	APC-related protein involved in embryogenesis and vulval development, regulation of Wnt signalling pathway, and regulation of multicellular organismal development.
alp-1	APLP1	Exon Skipping	APP family member of proteins that facilitates heparin binding activity and transition metal ion binding activity. Involved in body morphogenesis, ecdysis, collagen and cuticulin-based cuticle, and nematode larval development.
unc-70	HSPTB1	Exon Skipping	Facilitates actin filament binding activity and is involved in dendrite development, embryonic body morphogenesis, and muscle cell cellular homeostasis.
K04H4.2	N/A	Exon Skipping	Enables chitin binding activity.
unc-103	ENSP00000396900	Exon Skipping	Enables inward rectifier potassium channel activity. Involved in mating behaviour and regulation of muscle contraction.
zyg-12	HOOK1	Exon Skipping	Involved in centrosome localization, embryo development, and pronuclear migration.
mlt-11	TFPI	Exon Skipping	Serine-type endopeptidase inhibitor activity expressed in hypodermis.
daf-15	RPTOR	Alternative Splice Acceptor	Protein kinase activator and protein-macromolecule adaptor involved in dauer larval development, determination of adult lifespan, and regulation of autophagosome assembly. Expressed in the body wall musculature and pharyngeal muscle cell.
pat-12	N/A	Exon Skipping	Involved in embryonic morphogenesis and hemidesmosome assembly. Located in hemidesmosome.
ect-2	ECT2	Alternative Splice Acceptor	Epithelial cell transformation, cell fate determination, mitotic cytokinesis, and positive regulation of GTPase activity.
tim-1	TIMELESS	Alternative Splice Acceptor	DNA binding activity, embryo development, and sister chromatid cohesion.

Immunoprecipitation eluates were prepared for mass spectrometry-based proteomics using filter-aided sample preparation (FASP). Briefly, proteins were alkylated with iodoacetamide (IAA), buffer exchanged with urea followed by ammonium bicarbonate, and finally digested with Trypsin/Lys-C overnight at 37°C. After digestion, peptides were eluted from the FASP columns and subsequently desalted using C18 SPE cartridges (Waters) with a vacuum manifold. Desalted peptides were dried in a vacuum concentrator. Peptides were resuspended in H₂O/0.1% formic acid for LC-MS/MS analysis.

Peptides were separated using a 75 µm x 50 cm Acclaim™ PepMap™ 100 C18 reversed-phase-HPLC column (Thermo Scientific) on an Ultimate 3000 UHPLC (Thermo Scientific) with a 120-minute gradient (2–32% ACN with 0.1% formic acid) and analysed on a hybrid quadrupole-Orbitrap instrument (Q Exactive Plus, Thermo Fisher Scientific). Full MS survey scans were acquired at 70,000 resolution. The top 10 most abundant ions were selected for MS/MS analysis.

Raw data files were processed in MaxQuant (www.maxquant.org) and searched against the UniProt *Caenorhabditis elegans* protein sequence database. Search parameters

included constant modification of cysteine by carbamidomethylation and the variable modification, methionine oxidation. Proteins were identified using the filtering criteria of 1% protein and peptide false discovery rate.

3. Results

3.1. CCAR-1 regulates alternative splicing in *C. elegans*.

We used whole transcriptome RNA sequencing to examine the genome-wide alternative splicing changes with and without knock-out of CCAR-1 in *C. elegans*. The CCAR-1 deletion mutant strain VC1029 *ccar-1* (*gk433*) IV, which contains a deletion of the first three exons of the *ccar-1* gene resulting in a null mutant [33], was outcrossed three times with our laboratory wildtype N2 strain to create strain SDW040. RNA was extracted from wildtype N2 and CCAR-1 null (SDW040) worms on day 1 of adulthood in biological duplicate and sent for sequencing (Figure 1A). From the sequencing data, a VAST-Tools analysis was conducted to identify alternative splicing changes. We found 57,450 alternative splicing events (Supplementary Data 1), with 7133 significant changes (E[dPSI]<0.1 and

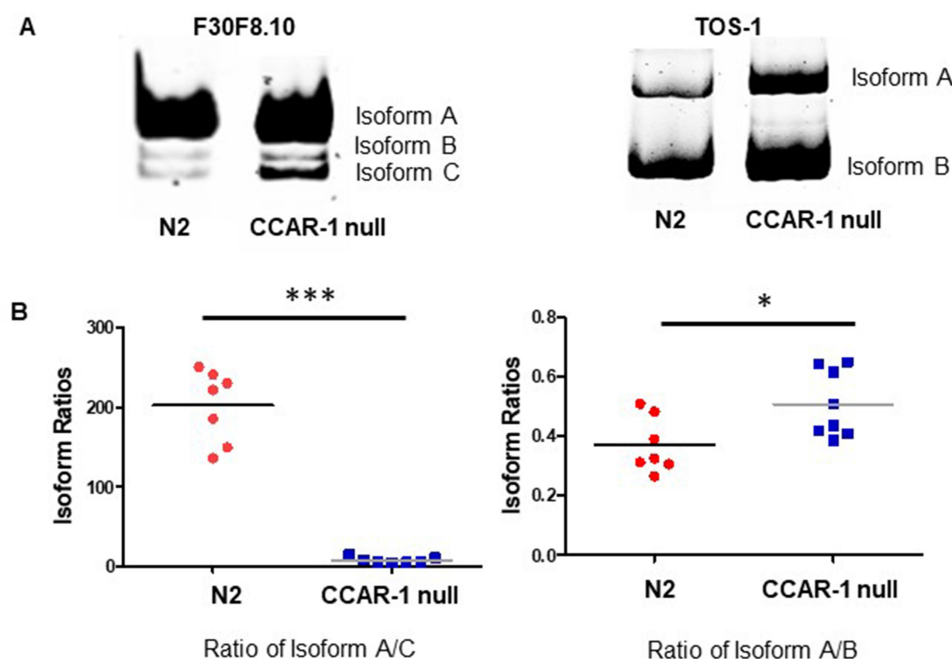


Figure 2. RT-PCR validation of alternatively spliced genes. This figure shows the RT391 PCR validation of CCAR-1-regulated alternative splicing from the RNA sequencing dataset. A. The RT-PCR images show the visual representation of isoform changes in the N2 and CCAR-1 null (SDW040) worms. B. The box plots represent the distribution of the isoform ratios of all populations of N2 and CCAR-1 null (SDW040) worms, N=7. The F30F8.10 box plot measures the ratio of isoform A to C and the *tos-1* box plot measures the ratio of isoform A to B. Based on a Mann-Whitney test, we recorded a p-value of 0.006 (***) for the F30F8.10 gene and a p-value of 0.0401 (*) for the *tos-1* gene.

MV [dPSI]>0). The majority of significant alternative splicing changes are due to exon skipping (4269), intron retention (1714), alternative splice donor (582), and alternative splice acceptor (568) (Figure 1B). We include a table of the top 20 significantly changing genes from the VAST-Tools analysis with information on the human homologs, the type of alternative splicing event, and the function (Table 1).

Next, we evaluated gene ontology by assessing the molecular functions and the biological processes of significantly changing genes from VAST-Tools using WormEnrichR (Supplementary Data 2). Key molecular functions such as DNA binding, actin binding, and RNA binding are altered with the deletion of CCAR-1 (Figure 1C). As for biological processes, the deletion of CCAR-1 regulates the splicing of genes involved in nematode larval development, the regulation of gene expression and embryo development (Figure 1D).

3.2. Validation of alternative splicing changes

To validate the alternative splicing changes found from the RNA sequencing, we used RT-PCR to examine two genes from our data set, *F30F8.10*, and *tos-1*. *F30F8.10* was among the top significantly changing genes in our dataset, and *tos-1* was a well-established splicing reporter in *C. elegans* studies [26,34]. From the RT-PCR, we determined the isoform ratios of these genes in N2 and CCAR-1 null (SDW040) worms. We further used Mann-Whitney tests to determine if the isoform changes were statistically significant.

F30F8.10 contains three alternatively spliced isoforms (A, B, and C) in both N2 and CCAR-1 null (SDW040). Notably, in the CCAR-1 null (SDW040), isoform B is upregulated (Figure 2A, top panel). We quantified the ratio between isoform A to C and checked for statistical significance between N2 and CCAR-1 null (SDW040) ratios (Supplementary Data 3). The isoform ratio was significantly decreased in SDW040 as compared to N2 with a p-value of < 0.006 (Figure 2A, lower panel).

Tos-1 gene contains five isoforms; however, here we focus on two isoforms, A and B, that showed substantial changes in both N2 and CCAR-1 null (SDW040) worms. We found that isoform A was upregulated in CCAR-1 null (SDW040) worms (Figure 2B). We quantified the ratio between isoform A to B and found that the ratio significantly increased in CCAR-1 null worms with a p-value of < 0.00401 (Figure 2B). Collectively, these results validate the RNA sequencing data and show that CCAR-1 regulates alternative splicing of previously unknown *C. elegans* genes.

3.3. Pulldown of CCAR-1 using mass spectrometry shows interaction with splicing factors UAF-1 and UAF-2

A previous study found that CCAR-1 regulation of alternative splicing requires binding to HRP-2 to facilitate alternative splicing changes [33]. To determine other interacting partners that CCAR-1 may work with to regulate splicing, we examined CCAR-1's interacting partners using mass spectrometry.

We constructed an *eft* promoter, GFP and FLAG-tagged *ccar-1* strain (peft:CCAR-1:GFP:3XFLAG) strain (SDW080) to pull down CCAR-1 for mass spectrometry. From the

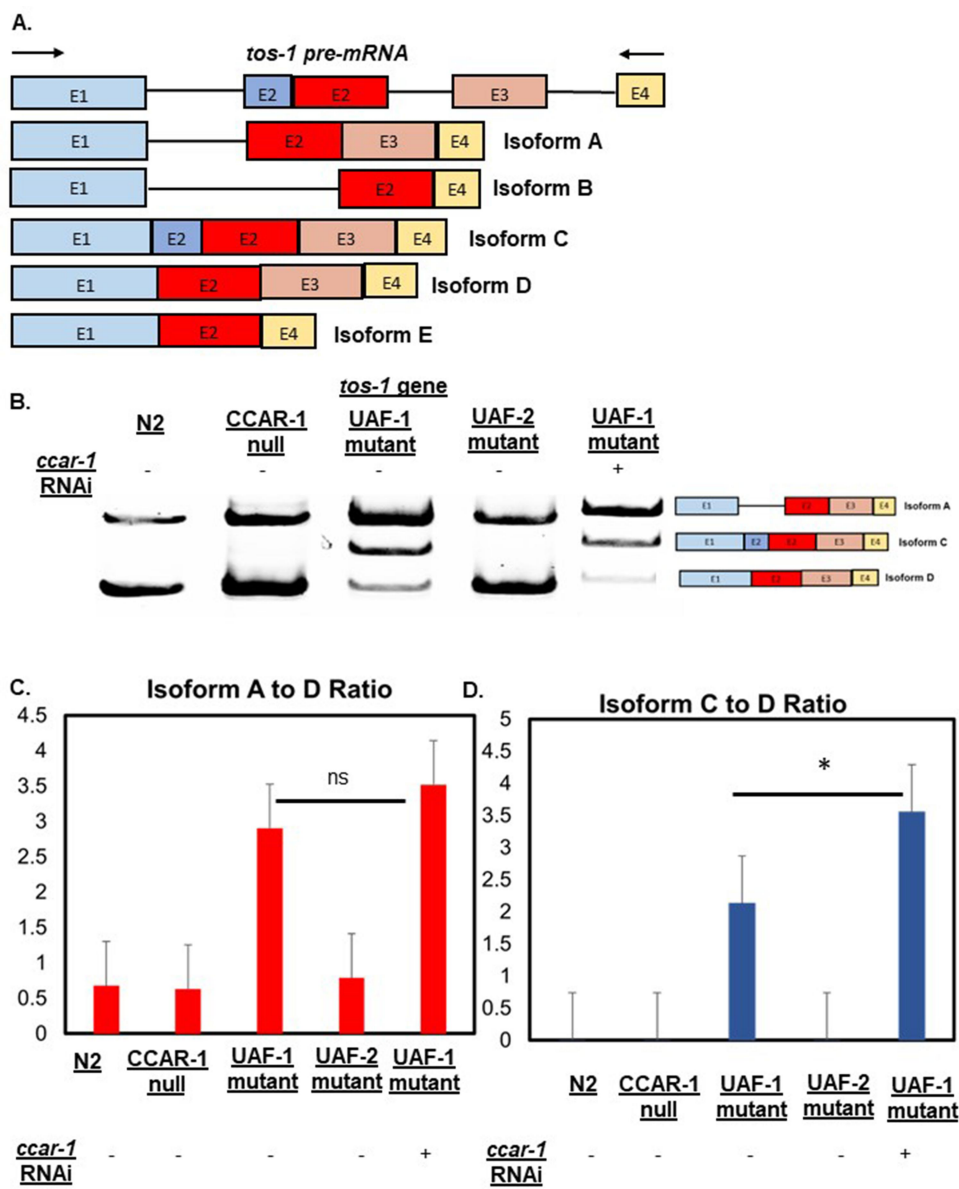


Figure 3. CCAR-1 RNAi affects the alternative splicing of the *tos-1* splicing reporter in UAF-1 mutants. A. Shows the *tos-1* pre-mRNA and subsequent isoforms due to alternative splicing. B. The RT-PCR results of N2, CCAR-1 null (SDW040), UAF-2 mutant (VC3010), and UAF-1 mutant (MT16492) (with and without *ccar-1* RNAi). C. Shows the isoform ratios of isoform A to D in N2, CCAR-1 null (SDW040), UAF-2 mutant (VC3010), and UAF-1 mutant (MT16492) (with and without *ccar-1* RNAi). D. Shows the isoform ratios of isoform C to D in N2, CCAR-1 null (SDW040), UAF-2 mutant (VC3010), and UAF-1 mutant (MT16492) (with and without *ccar-1* RNAi). The error bars in C and D represent the standard error and variability of isoform ratios from different replicates.

mass spectrometry data, we were interested in splicing factors interacting with CCAR-1, as this protein does not have an RNA-binding domain. We detect splicing factors from our list of proteins (Supplementary Data 4) [35], and amongst these highlighted two spliceosome factors, UAF-1 and UAF-2, the *C. elegans* homologs to the mammalian large and small U2AF subunits, U2AF65 and U2AF35, respectively. Mammalian CCAR2 previously interacted with U2AF65 [36], therefore, based on this study and our mass spectrometry data we wanted to further evaluate this interaction of CCAR-1 with UAF-1 and UAF-2 in *C. elegans*.

3.4. CCAR-1 RNAi affects alternative splicing in UAF-1 mutant worms

To establish the mechanistic importance of the interaction of CCAR-1 with splicing factors UAF-1 and UAF-2 in the alternative splicing of *C. elegans* genes, we used a *tos-1* splicing reporter, previously used to test UAF-1 splicing regulation [26,34,37]. We examined whether the knockdown of *ccar-1* affects the alternative splicing of the *tos-1* gene in UAF-1 and UAF-2 mutant backgrounds by quantifying the isoform ratios. The *tos-1* gene predominantly produces five isoforms (Figure 3A), however here we

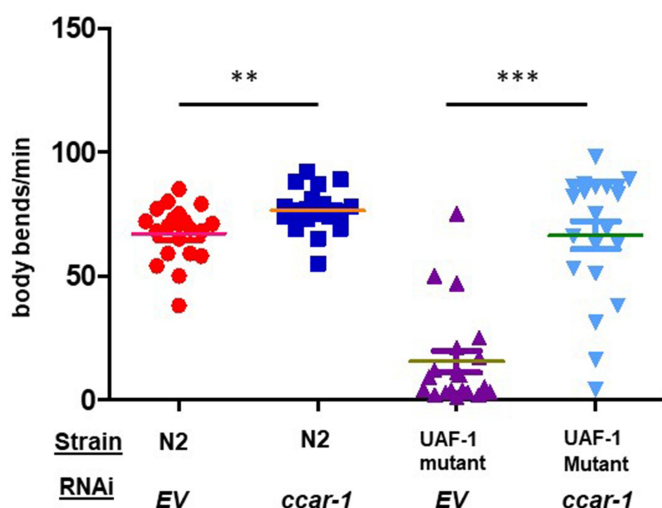


Figure 4. CCAR-1 RNAi rescues the motility of UAF-1 mutants. N2 and UAF-1 mutant (MT16492) grown at 25°C, were assessed for motility in a thrashing assay. Body bends per minute were measured for individual worms in an $N = 15$ for two biological replicates. Based on a Mann-Whitney test, we recorded a p-value of < 0.0057 between N2 EV and N2 *ccar-1* RNAi and a p-value of < 0.0001 between UAF-1 mutants (MT16492) EV and UAF-1 mutants (MT16492) *ccar-1* RNAi.

highlight three isoforms, A, C, and D, which are modified in our experiments. Isoform A contains an intron retention, isoform D contains partial exon skipping, and isoform C contains all exons, including full length exon 2, and has no intron retention (Figure 3A). We measured isoform A to D and isoform C to D ratios to determine *tos-1* isoform ratio changes.

We show that the CCAR-1 null (SDW040) and the UAF-2 mutant (VC3010) do not show significant differences between isoform ratios A to D or C to D compared to N2 (Figure 3B). However, the UAF-1 mutant (MT16492) shows a 6-fold change in isoform A to D ratio and up to a 30-fold change in isoform C to D compared to N2 (Figure 3C).

Then, to determine if CCAR-1 affects the alternative splicing pattern of the *tos-1* gene in the UAF-1 mutant strain (MT16492), we used *ccar-1* RNAi and assessed for isoform ratio changes in the *tos-1* splicing reporter. We observe that *ccar-1* RNAi significantly increases the isoform ratio of C to D in MT16492 worms by up to 2-fold (Figure 3D). The error bars represent the standard error and variability of isoform ratios from different replicates. This data suggests that *ccar-1* RNAi affects the splicing patterns of the *tos-1* gene in the UAF-1 mutant.

3.5. CCAR-1 RNAi significantly increases the motility of UAF-1 mutant worms

The *C. elegans* U2AF65 (*uaf-1*) and U2AF35 (*uaf-2*) genes cause genome-wide changes in 3' splice sites [34,38,39], and *uaf-1* mutants have embryonic viability and motility defects [26]. Thus, to further investigate if CCAR-1 works with UAF-1 to affect motility, we assessed movement in the N2 and

UAF-1 mutant (MT16492) worms using a thrashing assay previously used in *uaf-1* alternative splicing studies [26].

N2 and UAF-1 mutant (MT16492) worms were bleach synchronized and placed on EV (empty vector) and *ccar-1* RNAi plates at 25°C until development into day one adults. On day one of adulthood, we counted the number of body bends per minute for each worm and used a Mann-Whitney test to detect statistical significance. Consistent with our previous work [40], we show that *ccar-1* RNAi significantly increases the motility of N2 worms with a p-value of < 0.0057 . However, we also observe that *ccar-1* RNAi significantly rescues motility in the UAF-1 mutants (MT16492) strain with a p-value of < 0.0001 (Figure 4). This further suggested that the two proteins could be working together.

3.6. CCAR-1 RNAi significantly decreases the number of PolyQ aggregates in *uaf-1* RNAi-treated worms

Our previous work demonstrates that the knockdown of *ccar-1* by RNAi upregulates proteostasis, in a *sir-2.1* dependent manner, by decreasing polyglutamine aggregate formation in a *C. elegans* Huntington's disease model [40]. Also, from our alternative splicing analysis, we show that the knockdown of CCAR-1 regulates the alternative splicing of various small heat shock proteins (Supplementary Data 1). To determine if CCAR-1 is working with UAF-1 to regulate proteostasis, perhaps through effects on the splicing of genes such as chaperones, we assessed polyglutamine aggregate formation in response to empty vector, *ccar-1*, *uaf-1*, and *ccar-1/uaf-1* RNAi in a Huntington's disease model strain AM140 rmls132 (*unc-54p::Q35::YFP*) (Figure 5). AM140 strain contains 35 polyglutamine repeats fused to YFP (Q35:YFP) under the control of a muscle-specific promoter, which develops aggregates in the body wall muscle [25].

AM140 worms were bleach synchronized and grown in respective RNAi plates until day 3 of adulthood. Fluorescent images, as well as quantification of aggregates, are shown. As expected, we see an average of 17 aggregates/worm in empty vector (control) worms and a significantly lower average (p-value < 0.0001) of 12 aggregates/worm in *ccar-1* RNAi-treated worms [40]. In *uaf-1* RNAi-treated worms, we see an average of 18 aggregates/worm, slightly more than the N2 control. However, if we knock down *ccar-1* and *uaf-1* simultaneously, the average is reduced to 11 aggregates/worm, significantly reducing the number of aggregates per worm ($p < 0.0001$). These results show that CCAR-1 restores proteostasis in the Huntington's *C. elegans* disease model with UAF-1 RNAi and suggest that CCAR-1 is working together with spliceosome factor UAF-1 for this effect.

4. Discussion

Mammalian and *C. elegans* CCAR family members regulate the alternative splicing of genes [24,33]. However, there is a gap in knowledge of how this regulation occurs at the genome-wide level in a whole model organism. To address this, we used RNA sequencing and mass spectrometry to show

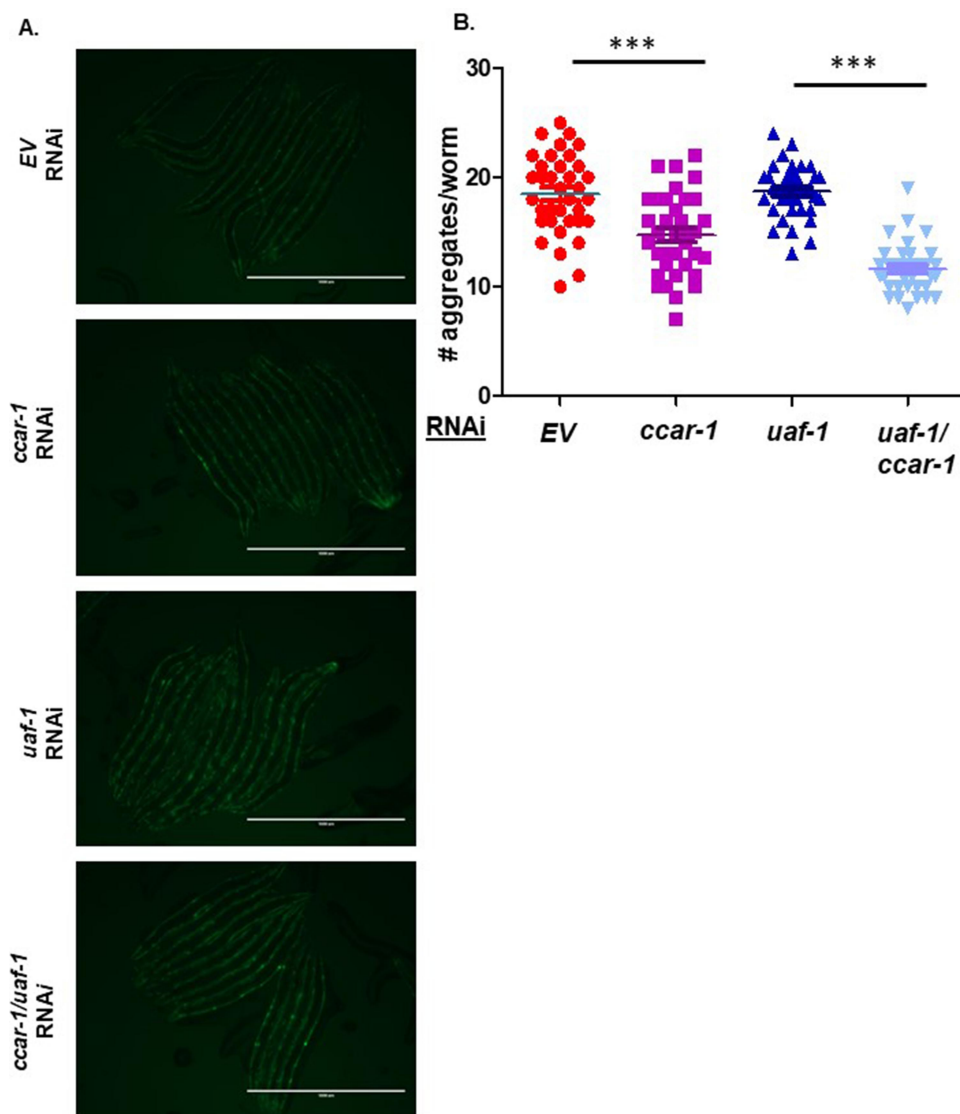


Figure 5. *Ccar-1* and *uaf-1* RNAi significantly decrease polyglutamine aggregation. A. Shows the fluorescent images of AM140 (Q35:YFP) fed control, *ccar-1*, *uaf-1*, and *ccar-1/uaf-1* RNAi from L1 larval stage to day 3 of adulthood. B. Shows quantification of the number of aggregates per worm in each condition with an $N=40$. Based on a Mann-Whitney test, we recorded a p-value of 0.0001 (***) between AM140 empty vector (EV) and AM140 *ccar-1* RNAi, and a p-value of 0.0001 (***) between AM140 *uaf-1*, and AM140 *uaf-1/ccar-1* RNAi.

new targets of CCAR-1 alternative splicing and the potential mechanism of action of alternative splicing.

We identify new alternative splicing targets of CCAR-1 with a variety of functions in the cell. We also found new interacting partners of *C. elegans* CCAR-1, including members of the spliceosome, UAF-1, and UAF-2. We show that *ccar-1* RNAi affects the *tos-1* splicing reporter in a UAF-1 mutant background and that CCAR-1 and UAF-1 work oppositely in the biological endpoints of motility and proteostasis in the worm. Overall, we demonstrate that CCAR-1 works with UAF-1 to regulate alternative splicing and physiological effects in *C. elegans*.

We provide a comprehensive list of alternative splicing changes occurring with the knockout of CCAR-1, mostly through exon skipping events (Supplementary data 1). Notably, we see alternative acceptor sites, that are previously linked to UAF-1 function in *C. elegans* [34]. Our dataset

identifies biological functions that have been earlier linked to CCAR-1, such as nematode larval development, the regulation of gene expression, morphology of the epithelium, and embryo development [14,16,24,33,40]. This gives us confidence that our dataset is a true representation of biological functions related to CCAR-1, however, it was previously unknown that these functions were regulated by the alternative splicing of genes. Interestingly, we identified that a key molecular function affected by CCAR-1 deletion is the alternative splicing of RNA-binding genes. This regulation of RNA binding genes by CCAR-1 could be one way to explain its role in alternative splicing.

A previous *C. elegans* study found that CCAR-1 is a splicing regulator of the structural gene *unc-52* [33]. Here, we identify other structural genes such as *apl-1*, *ketn-1*, and *vab-10* to be alternatively spliced by CCAR-1 and show various structural genes in the top significantly alternatively

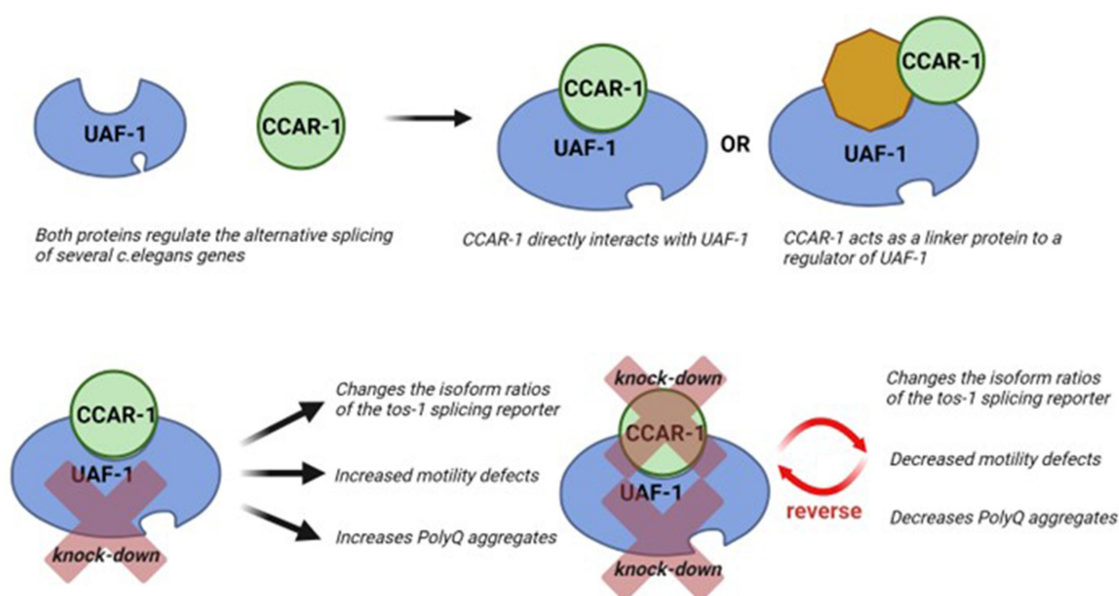


Figure 6. A model of the mechanism of action of alternative splicing regulation by CCAR-1 and UAF-1 in *C. elegans*.

spliced genes with deletion of *ccar-1* (Table 1). Our findings suggest that CCAR-1 has a larger role in regulating the alternative splicing of structural genes in *C. elegans*, which most have human homologs. There is an emerging interest in understanding the alternative splicing of structural genes since many of them are alternatively spliced during biogenesis [41,42]. Also, studies show that cancers associated with CCAR family members are epithelial-related and occur in hemidesmosome-related tissues [18,43–47]. In the future, it would be informative to examine the role of CCAR-1 in alternative splicing of epithelial genes during tumour progression.

Interestingly, our mass spectrometry data identifies the splicing factors UAF-1 and UAF-2 as interacting partners of CCAR-1. UAF-1 and UAF-2 are splicing factors of the spliceosome and aid snRNA U2 interaction with the intron, binding the polypyrimidine tract and recognizing the AG nucleotide on the 3' end of the intron [8,26,34,38,39]. The *C. elegans* UAF-1 mutant MT16492 *uaf-1*(n4588) III and UAF-2 mutant VC3010 *uaf-2* (gk3159) IV cause genome-wide changes in 3' splice site [34,38,39], and *uaf-1* (n4588) III mutants have embryonic viability and motility defects [26]. Additionally, a previous study investigating human protein-protein interactions of core and non-core spliceosome factors identified CCAR1 as an interaction partner of U2AF2/U2AF65 [36].

We speculate that CCAR-1 could negatively regulate UAF-1's function in alternative splicing in *C. elegans*, directly, or indirectly as a linker protein to a regulator of UAF-1 (Figure 6). This opposite regulation of CCAR-1 to UAF-1 alternative splicing could explain the contrasting functioning in a *tos-1* splicing reporter and motility defects (Figure 6). There is also still the possibility that CCAR-1 can bind directly to RNA to regulate splicing. CCAR-1 contains an S1-like domain, which is a putative RNA binding domain, which could be used for this purpose [13]. More research is needed to determine if CCAR-1 can bind to and regulate RNA directly. Future work to uncover the mechanism behind

CCAR-1 and UAF-1's combined role in alternative splicing will help elucidate novel roles for the CCAR family. Importantly, there is a need for further characterization of this mechanism of action by direct interaction experiments, such as immunoprecipitation, to test whether the interested proteins directly interact.

Lastly, using the worm's advantages, which are the availability of splicing factor mutants and the ability to examine physiological effects at the organismal level, we show that *ccar-1* RNAi affects *tos-1* gene splicing patterns in a UAF-1 mutant background. Furthermore, we show that *ccar-1* RNAi rescues the motility of the worms and reduces the number of aggregates in a Huntington's disease model worm. In both assays we see that CCAR-1 and UAF-1 are working oppositely, hence the hypothesis that CCAR-1 could be directly or indirectly negatively regulating UAF-1 function (Figure 6). Lastly, our RNA-Seq dataset shows that CCAR-1 regulates the alternative splicing of several small heat shock proteins, which could be a way to explain its role in proteostasis (Supplementary Data 1).

Collectively, our work identifies a larger role for CCAR-1 in the alternative splicing of *C. elegans* genes, other than *unc-52*, that could be directly or indirectly through the regulation of UAF-1. Future studies are needed to determine the precise mechanism of how CCAR-1 works with UAF-1 to regulate alternative splicing and how this interaction could affect these global splicing changes. Also, in future work, there is need for long-read sequencing techniques to identify more targets, including longer isoforms.

Acknowledgments

The wild-type Bristol N2, CCAR-1 mutant VC1029 *ccar-1* (gk433) IV, UAF-1 mutant MT16492 *uaf-1*(n4588) III, UAF-2 mutant VC3010 *uaf-2* (gk3159) IV, AM140 *rmls132* (*unc-54p:Q35:YFP*) strains were provided by the CGC, which is funded by NIH Office of Research Infrastructure Programs (P40 OD010440). This work was funded by NIH grant AG052149.

Data availability statement

The data that supports the findings of this study are openly available in the Sequence Read Archive (SRA) website <https://submit.ncbi.nlm.nih.gov/subs/sra>, reference number SUB8460771.

Disclosure statement

No potential conflict of interest was reported by the authors.

Funding

This work was funded by NIH grant R15 AG052149/AG/NIA NIH.

References

- Baralle FE, Giudice J. Alternative splicing as a regulator of development and tissue identity. *Nat Rev Mol Cell Biol.* 2017;18(7):437–451. doi: [10.1038/nrm.2017.27](https://doi.org/10.1038/nrm.2017.27)
- Jiang W, Chen L. Alternative splicing: human disease and quantitative analysis from high-throughput sequencing. *Comput Struct Biotechnol J.* 2021;19:183–195. doi: [10.1016/j.csbj.2020.12.009](https://doi.org/10.1016/j.csbj.2020.12.009)
- Liu XX, Guo Q-H, Xu W-B, et al. Rapid Regulation of Alternative Splicing in Response to Environmental Stresses. *Front Plant Sci.* 2022;13:832177. doi: [10.3389/fpls.2022.832177](https://doi.org/10.3389/fpls.2022.832177)
- Biamonti G, Caceres JF. Cellular stress and RNA splicing. *Trends Biochem Sci.* 2009;34(3):146–153. doi: [10.1016/j.tibs.2008.11.004](https://doi.org/10.1016/j.tibs.2008.11.004)
- Halleger M, Llorian M, and Smith CW. Alternative splicing: global insights. *FEBS J.* 2010;277(4):856–66. doi: [10.1111/j.1742-4658.2009.07521.x](https://doi.org/10.1111/j.1742-4658.2009.07521.x)
- Kim E, Goren A, Ast G. Alternative splicing and disease. *RNA Biol.* 2008;5(1):17–9. doi: [10.4161/rna.5.1.5944](https://doi.org/10.4161/rna.5.1.5944)
- Ramani AK, Calarco JA, Pan Q, et al. Genome-wide analysis of alternative splicing in *Caenorhabditis elegans*. *Genome Res.* 2011;21(2):342–348. doi: [10.1101/gr.114645.110](https://doi.org/10.1101/gr.114645.110)
- Zahler AM. Alternative splicing in *C. elegans*. *WormBook.* 2005;1–13. doi: [10.1895/wormbook.1.31.1](https://doi.org/10.1895/wormbook.1.31.1)
- Zahler AM. Pre-mRNA splicing and its regulation in *Caenorhabditis elegans*. *WormBook.* 2012;1–21. doi: [10.1895/wormbook.1.31.2](https://doi.org/10.1895/wormbook.1.31.2)
- Zhang Y, Qian J, Gu C, et al. Alternative splicing and cancer: a systematic review. *Sig Transduct Target Ther.* 2021;6(1):78. doi: [10.1038/s41392-021-00486-7](https://doi.org/10.1038/s41392-021-00486-7)
- Dutertre M, Sanchez G, Barbier J, et al. The emerging role of pre-messenger RNA splicing in stress responses: sending alternative messages and silent messengers. *RNA Biol.* 2011;8(5):740–7. doi: [10.4161/rna.8.5.16016](https://doi.org/10.4161/rna.8.5.16016)
- Anantharaman V, Aravind L. Analysis of DBC1 and its homologs suggests a potential mechanism for regulation of sirtuin domain deacetylases by NAD metabolites. *Cell Cycle.* 2008;7(10):1467–1472. doi: [10.4161/cc.7.10.5883](https://doi.org/10.4161/cc.7.10.5883)
- Brunquell J, Yuan J, Erwin A, et al. DBC1/CCAR2 and CCAR1 are largely disordered proteins that have evolved from one common ancestor. *Biomed Res Int.* 2014;2014:1–13. doi: [10.1155/2014/418458](https://doi.org/10.1155/2014/418458)
- Kim JE, Chen J, Lou Z. DBC1 is a negative regulator of SIRT1. *Nature.* 2008;451(7178):583–586. doi: [10.1038/nature06500](https://doi.org/10.1038/nature06500)
- Kim W, Ryu J, Kim JE. CCAR2/DBC1 and Hsp60 positively regulate expression of survivin in neuroblastoma cells. *Int J Mol Sci.* 2019;20(1):20(1). doi: [10.3390/ijms20010131](https://doi.org/10.3390/ijms20010131)
- Li Z, Chen L, Kabra N, et al. Inhibition of SUV39H1 methyltransferase activity by DBC1. *J Biol Chem.* 2009;284(16):10361–10366. doi: [10.1074/jbc.M900956200](https://doi.org/10.1074/jbc.M900956200)
- Raynes R, Pombier KM, Nguyen K, et al. The SIRT1 modulators AROS and DBC1 regulate HSF1 activity and the heat shock response. *PLoS One.* 2013;8(1):e54364. doi: [10.1371/journal.pone.0054364](https://doi.org/10.1371/journal.pone.0054364)
- Xu B, Li Q, Chen N, et al. The LIM protein Ajuba recruits DBC1 and CBP/p300 to acetylate ER α and enhances ER α target gene expression in breast cancer cells. *Nucleic Acids Res.* 2019;47(5):2322–2335. doi: [10.1093/nar/gky1306](https://doi.org/10.1093/nar/gky1306)
- Zhao W, Kruse J-P, Tang Y, et al. Negative regulation of the deacetylase SIRT1 by DBC1. *Nature.* 2008;451(7178):587–590. doi: [10.1038/nature06515](https://doi.org/10.1038/nature06515)
- Kong S, Dong H, Song J, et al. Deleted in breast cancer 1 suppresses B cell activation through RelB and is regulated by IKK α phosphorylation. *J Immunol.* 2015;195(8):3685–93. doi: [10.4049/jimmunol.1500713](https://doi.org/10.4049/jimmunol.1500713)
- Tong B, Hornak AJ, Maison SF, et al. Oncomodulin, an EF-Hand Ca $^{2+}$ Buffer, is critical for maintaining cochlear function in mice. *J Neurosci.* 2016;36(5):1631–1635. doi: [10.1523/JNEUROSCI.3311-15.2016](https://doi.org/10.1523/JNEUROSCI.3311-15.2016)
- Kolobynina KG, Solovyova VV, Levay K, et al. Emerging roles of the single EF-hand Ca $^{2+}$ sensor tescalcin in the regulation of gene expression, cell growth and differentiation. *J Cell Sci.* 2016;129(19):3533–3540. doi: [10.1242/jcs.191486](https://doi.org/10.1242/jcs.191486)
- Guo W, Sun B, Xiao Z, et al. The EF-hand Ca $^{2+}$ binding domain is not required for cytosolic Ca $^{2+}$ activation of the cardiac ryanodine receptor. *J Biol Chem.* 2016;291(5):2150–2160. doi: [10.1074/jbc.M115.693325](https://doi.org/10.1074/jbc.M115.693325)
- Close P, East P, Dirac-Svejstrup AB, et al. DBIRD complex integrates alternative mRNA splicing with RNA polymerase II transcript elongation. *Nature.* 2012;484(7394):386–389. doi: [10.1038/nature10925](https://doi.org/10.1038/nature10925)
- van Oosten-Hawle P, Porter RS, Morimoto RI. Regulation of organismal proteostasis by transcellular chaperone signaling. *Cell.* 2013;153(6):1366–78. doi: [10.1016/j.cell.2013.05.015](https://doi.org/10.1016/j.cell.2013.05.015)
- Gao X, Teng Y, Luo J, et al. The survival motor neuron gene *smn-1* interacts with the U2AF large subunit gene *uaf-1* to regulate *Caenorhabditis elegans* lifespan and motor functions. *RNA Biol.* 2014;11(9):1148–60. doi: [10.4161/rna.36100](https://doi.org/10.4161/rna.36100)
- Irimia M, Weatheritt R, Ellis JD, et al. A highly conserved program of neuronal microexons is misregulated in autistic brains. *Cell.* 2014;159(7):1511–23. doi: [10.1016/j.cell.2014.11.035](https://doi.org/10.1016/j.cell.2014.11.035)
- Tapial J, Ha KCH, Sterne-Weiler T, et al. An atlas of alternative splicing profiles and functional associations reveals new regulatory programs and genes that simultaneously express multiple major isoforms. *Genome Res.* 2017;27(10):1759–1768. doi: [10.1101/gr.220962.117](https://doi.org/10.1101/gr.220962.117)
- Torres-Mendez A, Bonnal S, Marquez Y, et al. A novel protein domain in an ancestral splicing factor drove the evolution of neural microexons. *Nat Ecol Evol.* 2019;3(4):691–701. doi: [10.1038/s41559-019-0813-6](https://doi.org/10.1038/s41559-019-0813-6)
- Chen EY, Tan CM, Kou Y, et al. Enrichr: interactive and collaborative HTML5 gene list enrichment analysis tool. *BMC Bioinf.* 2013;14(1):128. doi: [10.1186/1471-2105-14-128](https://doi.org/10.1186/1471-2105-14-128)
- Kuleshov MV, Jones MR, Rouillard AD, et al. Enrichr: a comprehensive gene set enrichment analysis web server 2016 update. *Nucleic Acids Res.* 2016;44(W1):W90–7. doi: [10.1093/nar/gkw377](https://doi.org/10.1093/nar/gkw377)
- Vu NT, Park MA, Shultz JC, et al. hnRNP U enhances caspase-9 splicing and is modulated by AKT-dependent phosphorylation of hnRNP L. *J Biol Chem.* 2013;288(12):8575–8584. doi: [10.1074/jbc.M112.443333](https://doi.org/10.1074/jbc.M112.443333)
- Fu R, Zhu Y, Jiang X, et al. CCAR-1 affects hemidesmosome biogenesis by regulating unc-52/perlecan alternative splicing in the *C. elegans* epidermis. *J Cell Sci.* 2018;131(11). doi: [10.1242/jcs.214379](https://doi.org/10.1242/jcs.214379)
- Ma L, Horvitz HR, Kim SK. Mutations in the *Caenorhabditis elegans* U2AF large subunit UAF-1 alter the choice of a 3' splice site in vivo. *PLoS Genet.* 2009;5(11):e1000708. doi: [10.1371/journal.pgen.1000708](https://doi.org/10.1371/journal.pgen.1000708)

- [35] Caudron-Herger M, Jansen RE, Wassmer E, et al. RBP2GO: a comprehensive pan-species database on RNA-binding proteins, their interactions and functions. *Nucleic Acids Res.* 2021;49(D1):D425–D436. doi: [10.1093/nar/gkaa1040](https://doi.org/10.1093/nar/gkaa1040)
- [36] Yu W, He L-R, Zhao Y-C, et al. Dynamic protein-protein interaction subnetworks of lung cancer in cases with smoking history. *Chin J Cancer.* 2012;32(2):84–90. doi: [10.5732/cjc.012.10099](https://doi.org/10.5732/cjc.012.10099)
- [37] Ma L, Gao X, Luo J, et al. The *Caenorhabditis elegans* gene *mfap-1* encodes a nuclear protein that affects alternative splicing. *PLoS Genet.* 2012;8(7):e1002827. doi: [10.1371/journal.pgen.1002827](https://doi.org/10.1371/journal.pgen.1002827)
- [38] Hollins C, ZORIO DAR, MACMORRIS M, et al. U2AF binding selects for the high conservation of the *C. elegans* 3' splice site. *RNA.* 2005;11(3):248–53. doi: [10.1261/rna.7221605](https://doi.org/10.1261/rna.7221605)
- [39] Kielkopf CL, Lucke S, Green MR. U2AF homology motifs: protein recognition in the RRM world. *Genes Dev.* 2004;18(13):1513–1526. doi: [10.1101/gad.1206204](https://doi.org/10.1101/gad.1206204)
- [40] Brunquell J, Raynes R, Bowers P, et al. CCAR-1 is a negative regulator of the heat-shock response in *Caenorhabditis elegans*. *Aging Cell.* 2018;17(5):e12813. doi: [10.1111/accel.12813](https://doi.org/10.1111/accel.12813)
- [41] Lundquist EA, Herman RK. The *mec-8* gene of *Caenorhabditis elegans* affects muscle and sensory neuron function and interacts with three other genes: *unc-52*, *smu-1* and *smu-2*. *Genetics.* 1994;138(1):83–101. doi: [10.1093/genetics/138.1.83](https://doi.org/10.1093/genetics/138.1.83)
- [42] Sugaya K, Hongo E, Ishihara Y, et al. The conserved role of *Smu1* in splicing is characterized in its mammalian temperature-sensitive mutant. *J Cell Sci.* 2006;119(23):4944–51. doi: [10.1242/jcs.03288](https://doi.org/10.1242/jcs.03288)
- [43] Muthu M, Somagani J, Cheriyan VT, et al. Identification and testing of novel CARP-1 functional mimetic compounds as inhibitors of non-small cell lung and triple negative breast cancers. *J Biomed Nanotechnol.* 2015;11(9):1608–1627. doi: [10.1166/jbn.2015.2099](https://doi.org/10.1166/jbn.2015.2099)
- [44] Colman L, Caggiani M, Leyva A, et al. The protein deleted in breast cancer-1 (DBC1) regulates vascular response and formation of aortic dissection during angiotensin II infusion. *Sci Rep.* 2020;10(1):6772. doi: [10.1038/s41598-020-63841-8](https://doi.org/10.1038/s41598-020-63841-8)
- [45] Fang Q, Bellanti JA, Zheng SG. Advances on the role of the deleted in breast cancer (DBC1) in cancer and autoimmune diseases. *J Leukocyte Biol.* 2021;109(2):449–454. doi: [10.1002/JLB.6MR0320-086R](https://doi.org/10.1002/JLB.6MR0320-086R)
- [46] Muthu M, Cheriyan VT, Rishi AK. CARP-1/CCAR1: a biphasic regulator of cancer cell growth and apoptosis. *Oncotarget.* 2015;6(9):6499–510. doi: [10.18632/oncotarget.3376](https://doi.org/10.18632/oncotarget.3376)
- [47] Santos L, Colman L, Contreras P, et al. A novel form of deleted in breast cancer 1 (DBC1) lacking the N-terminal domain does not bind SIRT1 and is dynamically regulated in vivo. *Sci Rep.* 2019;9(1):14381. doi: [10.1038/s41598-019-50789-7](https://doi.org/10.1038/s41598-019-50789-7)